

Chirp-Permuted AFDM for Quantum-Resilient Physical-Layer Secure Communications

Hyeon Seok Rou[®], *Member, IEEE*, Giuseppe Thadeu Freitas de Abreu[®], *Senior Member, IEEE*.

Abstract—This article presents a novel physical-layer secure communications scheme based on the recently discovered chirp-permuted affine frequency division multiplexing (AFDM) waveform, which results in a completely different received signal to the eavesdropper with the incorrect chirp-permutation order, even under co-located eavesdropping with perfect channel information. The security of the proposed scheme is studied in terms of the complexity required to find the correct permutation via classical and quantum search algorithms, which are shown to be infeasible due to the factorially-scaling search space, as well as theoretical and simulated analyses of a random-guess approach, indicating an infeasible probability of breach by chance.

Index Terms—physical-layer, quantum-resilient security, B5G, wireless communications, chirp-permutation, AFDM.

I. INTRODUCTION

The rapid evolution of wireless communications technologies, transitioning towards beyond-fifth-generation (B5G) and sixth-generation (6G) networks, is significantly increasing performances in terms of data rates, latency, and device connectivity, in addition to enabling new functionalities such as edge computing, integrated artificial intelligence (AI), and integrated sensing and communications (ISAC) [1]–[3].

The penetration of these innovations into use cases such as critical mission, autonomous vehicles, and Internet-of-Things (IoT) are, however, also expected to increase the exposure to security threats [4], which makes inherent and resilient security a must-have feature in future networks. Indeed, traditional cryptographic methods, although effective in the current technological paradigm, are expected to face significant challenges with the rise of quantum computing, which can efficiently break widely-used public key cryptosystems such as the RSA and ECC, via accelerated quantum algorithms [5]. This has motivated the investigation of physical layer security [6], [7] and quantum-resilient cryptography [8], [9] to ensure the security and privacy of future wireless systems.

Physical layer security leverages the unique characteristics of the wireless medium, such as fading, interference, and waveform modulation patterns, to introduce an additional layer of protection against eavesdropping and other adversarial attacks. Complementing these efforts, quantum-resilient cryptography have been investigated to develop secure communications algorithms that are resistant to quantum computing-based eavesdropping and attacks, which are known for their efficiency in solving previously prohibitive complex mathematical

problems, such as factoring large numbers or searching a large codebook [10], exponentially faster than classical computers, consequently threatening traditional encryption schemes. To address this challenge, post-quantum cryptographic schemes, such as hash- and multivariate quadratic-based algorithms, have gained attention as a means to ensure that encryption remains secure and unbreakable even against quantum-accelerated factorization and search algorithms [8].

In light of the above, this article proposes an efficient physical-layer secure communications scheme which is resilient even to quantum computer-based eavesdropping, leveraging a recently discovered chirp-permutation domain [11] of a next-generation waveform - affine frequency division multiplexing (AFDM) [12] known for its high performance over doubly-dispersive channels, in order to enable security and resilience in the B5G and post-quantum 6G systems. The contributions of the article can be summarized as follows:

- A secure communications scheme based on the chirp-permuted AFDM is proposed, resulting in a completely undecodable received signal to the eavesdropper with the incorrect chirp-permutation order, even under co-located eavesdropping with perfect channel information.
- The security of the proposed scheme against eavesdroppers employing either a classical or quantum-accelerated searches, or a random guess approach, is studied via numerical analysis and simulation, which demonstrate that the computational complexity required to find the correct permutation is infeasible even to quantum computers and even for systems with a small number of subcarriers, and that the likelihood of data detection by chance is extremely low even with a significantly close guess.

II. SYSTEM MODEL

Consider a communications scenario with transmitter Alice, legitimate receiver Bob, and eavesdropper Eve, all equipped with single antennas. Alice wishes to securely transmit data to Bob over the wireless channel, while ensuring that Eve is unable to decode the transmitted data.

The Alice-to-Bob and Alice-to-Eve wireless channels are modeled as doubly-dispersive channels with unique delay-Doppler profiles [13], which is elaborated in the sequel. It is assumed that Alice is not equipped with the channel state information (CSI) of either channels, such that CSI-based precoded encryption techniques are not possible. On the other hand, it is assumed that both Bob and Eve has perfect CSI of their respective channels. Later, we will also consider the extreme case where Bob and Eve are co-located, such that Eve has the same CSI as Bob, and receives the exact same signal.

Hyeon Seok Rou and Giuseppe Thadeu Freitas de Abreu are with the School of Computer Science and Engineering, Constructor University, Campus Ring 1, 28759 Bremen, Germany (emails: hrou@constructor.university, gfreu@constructor.university).

A. Received Signal Model over Doubly-Dispersive Channels

Consider a doubly-dispersive wireless channel between a single-input single-output (SISO) transmitter and a receiver described by P resolvable propagation paths, where each p -th scattering path induces a delay $\tau_p \in [0, \tau^{\max}]$ and Doppler shift $\nu_p \in [-\nu^{\max}, +\nu^{\max}]$ to the received signal. Then, the received signal sampled at a frequency of $f_s \triangleq \frac{1}{T_s}$, can be efficiently represented via the discrete circular convolutional channel model given by [13]

$$\mathbf{r} \triangleq \mathbf{H}\mathbf{s} + \mathbf{w} = \left(\sum_{p=1}^P h_p \cdot \Phi_p \cdot \mathbf{Z}^{f_p} \cdot \mathbf{\Pi}^{\ell_p} \right) \mathbf{s} + \mathbf{w} \in \mathbb{C}^{N \times 1}, \quad (1)$$

where $\mathbf{r} \in \mathbb{C}^{N \times 1}$, $\mathbf{s} \in \mathbb{C}^{N \times 1}$, and $\mathbf{w} \in \mathbb{C}^{N \times 1}$ are the discrete vectors of the received signal, transmit signal, and additive white Gaussian noise (AWGN) signal, respectively, $\ell_p \triangleq \lfloor \frac{\tau_p}{T_s} \rfloor \in \mathbb{N}_0$ and $f_p \triangleq \frac{N\nu_p}{f_s} \in \mathbb{R}$ are the normalized integer path delay and normalized digital Doppler shift of the p -th propagation path.

Each p -th path within the full circular convolutional matrix $\mathbf{H} \triangleq \sum_{p=1}^P h_p \Phi_p \mathbf{Z}^{f_p} \mathbf{\Pi}^{\ell_p} \in \mathbb{C}^{N \times N}$, is parametrized by the complex channel fading coefficient $h_p \in \mathbb{C}$, the diagonal prefix phase matrix $\Phi_p \in \mathbb{C}^{N \times N}$ with the waveform-specific prefix phase function $\phi(n)$, given by

$$\Phi_p \triangleq \text{diag}([e^{-j2\pi \cdot \phi(\ell_p)}, \dots, e^{-j2\pi \cdot \phi(1)}, \overbrace{1, \dots, 1}^{N-\ell_p \text{ ones}}]) \in \mathbb{C}^{N \times N}, \quad (2)$$

the diagonal roots-of-unity matrix $\mathbf{Z} \in \mathbb{C}^{N \times N}$ given by

$$\mathbf{Z} \triangleq \text{diag}([e^{-j2\pi \frac{0}{N}}, \dots, e^{-j2\pi \frac{N-1}{N}}]) \in \mathbb{C}^{N \times N}, \quad (3)$$

which is taken to the f_p -th power, and finally the right-multiplying circular left-shift matrix $\mathbf{\Pi} \in \mathbb{C}^{N \times N}$, taken to the ℓ_p -th integer power¹.

B. Affine Frequency Division Multiplexing (AFDM) Waveform

The recently proposed AFDM waveform is a novel modulation scheme that is designed to provide high spectral efficiency and full diversity over doubly-dispersive channels, using chirp-domain subcarriers and a lower modulation complexity than its competitors [12]. AFDM modulates a sequence of N symbols, $\mathbf{x} \in \mathcal{X}^{N \times 1}$, whose elements are drawn from an M -ary complex digital constellation $\mathcal{X} \subset \mathbb{C}$, unto the time domain signal using the inverse discrete affine Fourier transform (IDAFT),

$$\mathbf{s}^{\text{AFDM}} \triangleq \mathbf{A}^{-1} \mathbf{x} \in \mathbb{C}^{N \times 1}, \quad (4)$$

where the N -point forward discrete affine Fourier transform (DAFT) matrix $\mathbf{A} \in \mathbb{C}^{N \times N}$ and its inverse $\mathbf{A}^{-1} \in \mathbb{C}^{N \times N}$ are efficiently described in terms of a discrete Fourier transform (DFT) matrix and two diagonal chirp sequences, as

$$\mathbf{A} \triangleq \Lambda_{c_2} \mathbf{F}_N \Lambda_{c_1} \in \mathbb{C}^{N \times N}, \quad (5a)$$

$$\mathbf{A}^{-1} \triangleq (\Lambda_{c_2} \mathbf{F}_N \Lambda_{c_1})^{-1} = \Lambda_{c_1}^H \mathbf{F}_N^H \Lambda_{c_2}^H = \mathbf{A}^H \in \mathbb{C}^{N \times N}, \quad (5b)$$

where $\mathbf{F}_N \times \mathbb{C}^{N \times N}$ is the normalized N -point DFT matrix, and $\Lambda_{c_1} \triangleq \text{diag}(\boldsymbol{\lambda}_{c_1}) \in \mathbb{C}^{N \times N}$, $\Lambda_{c_2} \triangleq \text{diag}(\boldsymbol{\lambda}_{c_2}) \in \mathbb{C}^{N \times N}$ are diagonal chirp matrices whose elements are described by the chirp vector $\boldsymbol{\lambda}_{c_i} \triangleq [e^{-j2\pi c_i (0)^2}, \dots, e^{-j2\pi c_i (N-1)^2}] \in \mathbb{C}^{N \times 1}$ with a central digital frequency of c_i .

¹For the sake of conciseness, we refer readers to the full derivation and details of the doubly-dispersive channel model to [13].

The first chirp frequency c_1 must be optimized to achieve the full diversity characteristics of the AFDM waveform, which is obtained in closed-form given the maximum unambiguous Doppler shift f^{\max} of the channel and an arbitrary guard width $\xi \in \mathbb{N}_0$ of the waveform [12], as

$$c_1^{\text{opt}} = \frac{2(f^{\max} + \xi) + 1}{2N}. \quad (6)$$

On the other hand, the second chirp frequency c_2 , is a free parameter which does affect the performance of the AFDM, but only certain waveform properties such as the ambiguity function. This degree-of-freedom in the second chirp will be exploited in the proposed chirp-permuted AFDM-based secure communications scheme, described below.

III. PROPOSED SECURE COMMUNICATIONS SCHEME VIA CHIRP-PERMUTED AFDM

Given the above, we propose to permute the second chirp sequence Λ_{c_2} in the AFDM modulation and demodulation processes (*i.e.*, the DAFT and IDAFT), which will be shown to retain the full diversity delay-Doppler characteristics of the AFDM, but yield two completely different physical waveforms. This approach was leveraged in [11] to enable index modulation (IM) over the AFDM using the chirp-permutation domain codebook, and in this article, will be leveraged to provide physical-layer security against eavesdroppers.

A. Chirp-Permuted AFDM Waveform

Let the permutation operation of an arbitrary sequence of length N with order $i \in \{1, \dots, N!\}$ be denoted by $\text{perm}(\cdot, i)$, and the permutation order i is assumed to be in ascending order of the sequence element indices². Then, by defining the diagonal matrix formed from the i -th permutation of the second chirp sequence $\boldsymbol{\lambda}_{c_2}$ as

$$\Lambda_{c_2, i} \triangleq \text{diag}(\text{perm}(\boldsymbol{\lambda}_{c_2}, i)) \in \mathbb{C}^{N \times N}, \quad (7)$$

the i -th permuted DAFT and IDAFT matrices are given by

$$\mathbf{A}_i \triangleq \Lambda_{c_2, i} \mathbf{F}_N \Lambda_{c_1} \in \mathbb{C}^{N \times N}, \quad (8a)$$

$$\mathbf{A}_i^{-1} \triangleq \Lambda_{c_1}^H \mathbf{F}_N^H \Lambda_{c_2, i}^H \in \mathbb{C}^{N \times N}, \quad (8b)$$

which is still a linear unitary transform.

In all, the chirp-permuted (CP)-AFDM waveform with the i -th permutation order is given by

$$\mathbf{s}_i \triangleq \mathbf{A}_i^{-1} \mathbf{x} = \Lambda_{c_1}^H \mathbf{F}_N^H \Lambda_{c_2, i}^H \mathbf{x} \in \mathbb{C}^{N \times 1}. \quad (9)$$

B. Effective Channel Analysis of the Chirp-Permuted AFDM

The effective channel of the CP-AFDM waveform representing the input-output relationship of the transmit symbols \mathbf{x} , can be obtained under the demodulation with the matched permuted-DAFT matrix \mathbf{A}_i , as

$$\begin{aligned} \mathbf{G}_i &\triangleq \mathbf{A}_i \mathbf{H} \mathbf{A}_i^{-1} = (\Lambda_{c_2, i} \mathbf{F}_N \Lambda_{c_1}) \mathbf{H} (\Lambda_{c_1}^H \mathbf{F}_N^H \Lambda_{c_2, i}^H) \\ &= \Lambda_{c_2, i} \boldsymbol{\Xi} \Lambda_{c_2, i}^H \in \mathbb{C}^{N \times N}, \end{aligned} \quad (10)$$

where $\boldsymbol{\Xi} \triangleq \mathbf{F}_N \Lambda_{c_1} \mathbf{H} \Lambda_{c_1}^H \mathbf{F}_N^H \in \mathbb{C}^{N \times N}$ represents the intermediate effective channel before the second chirp domain.

²To provide an example, $\text{perm}([x_1, x_2, x_3, x_4], 1) = [x_1, x_2, x_3, x_4]$, $\text{perm}([x_1, x_2, x_3, x_4], 2) = [x_1, x_2, x_4, x_3]$, $\text{perm}([x_1, x_2, x_3, x_4], 3) = [x_1, x_3, x_2, x_4]$, $\text{perm}([x_1, x_2, x_3, x_4], 4) = [x_1, x_3, x_4, x_2]$, *etc.*

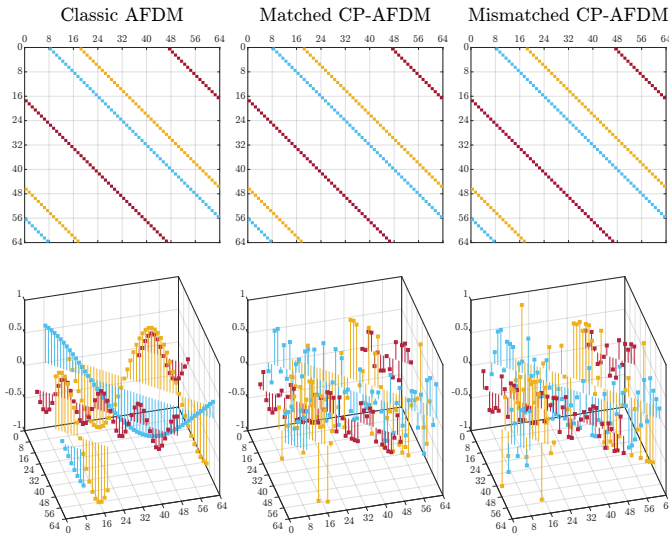


Fig. 1. Illustrations of the effective channels of AFDM and CP-AFDM waveforms, and permutation-mismatched CP-AFDM system of (12b), in 2D (highlighting channel structure) and 3D (highlighting channel coefficients).

The above formulation reveals an important property of chirp-permuted AFDM signals, and for AFDM waveforms in general³, which has been previously observed but not analyzed. As the second chirp (pre-chirp) operations Λ_{c_2} and $\Lambda_{c_2}^H$ are diagonal matrices, the induced effects are power scaling of the elements and only a similarity transformation onto the intermediate effective channel Ξ . In other words, the second chirp matrices (pre-chirp domain) cannot change the structure of the entire effective channel and therefore has no effect on the delay-Doppler orthogonality properties of the AFDM. Instead, the key delay-Doppler spreading property of the AFDM is only contained within the inner transformations via the post-chirp scaling Λ_{c_1} and the Fourier transform \mathbf{F}_N .

This behavior is clearly highlighted in Figure 1, where it can be seen that the CP-AFDM waveform results in an identical channel structure as the classic AFDM, and hence same delay-Doppler characteristics, but vastly different channel coefficients and consequently received signal.

C. Secure Communications Scheme

Finally, we propose the secure communications scheme based on the above-described CP-AFDM waveform, which enables quantum-resilient physical-layer security against eavesdroppers in a doubly-dispersive environment.

Assume that Alice and Bob share a predetermined secret key $k \in \{1, \dots, N!\}$, unknown to Eve, which is used to determine the permutation order of the chirp sequence in the CP-AFDM waveform. Alice transmits the data symbol vector $\mathbf{x} \in \mathbb{C}^{N \times 1}$ modulated via the CP-AFDM signal $\mathbf{s}_k \triangleq \mathbf{A}_k^{-1} \mathbf{x} \in \mathcal{X}^{N \times 1}$ with the secret chirp-permutation order k . The corresponding received signal at Bob and Eve are given by

$$\mathbf{r}_B \triangleq \mathbf{H}_B \mathbf{A}_k^{-1} \mathbf{x} + \mathbf{w}_B \in \mathbb{C}^{N \times 1}, \quad (11a)$$

$$\mathbf{r}_E \triangleq \mathbf{H}_E \mathbf{A}_k^{-1} \mathbf{x} + \mathbf{w}_E \in \mathbb{C}^{N \times 1}, \quad (11b)$$

where $\mathbf{w}_B \sim \mathcal{CN}(\mathbf{0}, \sigma_B^2 \mathbf{I}_N)$ and $\mathbf{w}_E \sim \mathcal{CN}(\mathbf{0}, \sigma_E^2 \mathbf{I}_N)$ are the AWGN vectors respectively at Bob and Eve, with noise variances σ_B^2 and σ_E^2 .

³The CP-AFDM reduces to the original AFDM of [12] with $i = 1$.

It is assumed that both Bob and Eve have perfect CSI of their respective channels, $\mathbf{H}_B \in \mathbb{C}^{N \times N}$ and $\mathbf{H}_E \in \mathbb{C}^{N \times N}$, such that they can perform equalization and decode the transmitted data. However, recall that only Bob has the correct permutation key $k \in \{1, \dots, N!\}$ and therefore the correct demodulator \mathbf{A}_k , while Eve does not have the correct permutation order, and must use some arbitrary key $k' \in \{1, \dots, N!\}$ and the corresponding demodulator $\mathbf{A}_{k'}$.

The demodulated signals are correspondingly given by

$$\mathbf{y}_B \triangleq \mathbf{A}_k \mathbf{r}_B = \mathbf{A}_k \mathbf{H}_B \mathbf{A}_k^{-1} \mathbf{x} + \mathbf{A}_k \mathbf{w}_B \in \mathbb{C}^{N \times 1}, \quad (12a)$$

$$\mathbf{y}_E \triangleq \mathbf{A}_{k'} \mathbf{r}_E = \mathbf{A}_{k'} \mathbf{H}_E \mathbf{A}_{k'}^{-1} \mathbf{x} + \mathbf{A}_{k'} \mathbf{w}_E \in \mathbb{C}^{N \times 1}, \quad (12b)$$

where the corresponding maximum likelihood (ML)-detected symbols are given by

$$\hat{\mathbf{x}}_B^{\text{ML}} \triangleq \underset{\mathbf{x} \in \mathcal{X}^{N \times 1}}{\text{argmin}} \|\mathbf{y}_B - \mathbf{A}_k \mathbf{H}_B \mathbf{A}_k^{-1} \mathbf{x}\|_2^2 \in \mathbb{C}^{N \times 1}, \quad (13a)$$

$$\hat{\mathbf{x}}_E^{\text{ML}} \triangleq \underset{\mathbf{x} \in \mathcal{X}^{N \times 1}}{\text{argmin}} \|\mathbf{y}_E - \mathbf{A}_{k'} \mathbf{H}_E \mathbf{A}_{k'}^{-1} \mathbf{x}\|_2^2 \in \mathbb{C}^{N \times 1}. \quad (13b)$$

Alternatively, the minimum mean-squared-error (MMSE) equalized symbols can be obtained by

$$\tilde{\mathbf{x}}_B^{\text{MMSE}} \triangleq \mathbf{A}_k (\mathbf{H}_B^H (\mathbf{H}_B \mathbf{H}_B^H + \sigma_B^2 \mathbf{I}_N)^{-1}) \mathbf{r}_B \in \mathbb{C}^{N \times 1}, \quad (14a)$$

$$\tilde{\mathbf{x}}_E^{\text{MMSE}} \triangleq \mathbf{A}_{k'} (\mathbf{H}_E^H (\mathbf{H}_E \mathbf{H}_E^H + \sigma_E^2 \mathbf{I}_N)^{-1}) \mathbf{r}_E \in \mathbb{C}^{N \times 1}. \quad (14b)$$

In addition, we also consider a special optimal case for Eve, where it is considered to be co-located with Bob, such that Eve has the same CSI as Bob, *i.e.*, $\mathbf{H}_E = \mathbf{H}_B$ and $\sigma_E^2 = \sigma_B^2$, and therefore assumed to receive the exact same signal as Bob, yielding respectively

$$\mathbf{y}_{E\text{-co}} \triangleq \mathbf{A}_{k'} \mathbf{r}_B = \mathbf{A}_{k'} \mathbf{H}_B \mathbf{A}_k^{-1} \mathbf{x} + \mathbf{A}_{k'} \mathbf{w}_B \in \mathbb{C}^{N \times 1}, \quad (15)$$

$$\hat{\mathbf{x}}_{E\text{-co}}^{\text{ML}} \triangleq \underset{\mathbf{x} \in \mathcal{X}^{N \times 1}}{\text{argmin}} \|\mathbf{y}_{E\text{-co}} - \mathbf{A}_{k'} \mathbf{H}_B \mathbf{A}_k^{-1} \mathbf{x}\|_2^2 \in \mathbb{C}^{N \times 1}, \quad (16)$$

$$\tilde{\mathbf{x}}_{E\text{-co}}^{\text{MMSE}} \triangleq \mathbf{A}_{k'} (\mathbf{H}_B^H (\mathbf{H}_B \mathbf{H}_B^H + \sigma_B^2 \mathbf{I}_N)^{-1}) \mathbf{r}_B \in \mathbb{C}^{N \times 1}, \quad (17)$$

where it can be seen by comparing the system corresponding to Bob in (12a), (13a), (14a) against co-located Eve in (15), (16), (17), the only difference lies in the permutation key k and k' , which is the only information that Eve does not have.

The effective channel of Eve with mismatched permutation key can be seen in Figure 1, where while the doubly-dispersive channel structure remains identical, the coefficients are vastly different between matched CP-AFDM ($k = k'$, at Bob) and the mismatched CP-AFDM ($k \neq k'$, at Eve), resulting in completely different received signals.

IV. SECURITY ANALYSIS

In this section, the security of the proposed scheme is analyzed by considering two key factors at the eavesdropper Eve: *a*) the computational hardness of the eavesdropper accurately determining the permutation key through exhaustive search, which is demonstrated to be infeasible even with aid of quantum computers, and *b*) the likelihood of successfully employing a random guess strategy of the permutation key, which is also shown to be practically infeasible, and its corresponding impact on the bit-error-rate (BER) performance.

A. Eavesdropper with Exhaustive Search Strategy

1) *Classical Computing Eavesdropper*: Given a system with N number of subcarriers, there trivially exist $N!$ number of possible permutation keys in the CP-AFDM scheme following (5) and (7). Consequently, an eavesdropper employing an exhaustive search must evaluate all $N!$ possible permutations to determine the correct permutation key $k \in \{1, \dots, N!\}$.

One approach would be to construct and evaluate the MMSE filter $\mathbf{M}_{k'} \triangleq \mathbf{A}_{k'}(\mathbf{H}_E^H(\mathbf{H}_E\mathbf{H}_E^H + \sigma_E^2\mathbf{I}_N)^{-1})$ for all valid permutation orders $k' \in \{1, \dots, N!\}$, and select the key with the lowest mean-squared-error (MSE) metric. Such approach would require a computational complexity of $\mathcal{O}(N! \cdot N^3)$, which is quickly dominated by $N!$ for even small values of N . For example, with only $N=16$, $N! \approx 2.1 \times 10^{13}$, whereas $N^3 = 4096$. Even idealistically considering a computational complexity of $\mathcal{O}(1)$ for each MSE or ML metric evaluation, the total complexity order is still $\mathcal{O}(N!)$, which is exponentially large and infeasible for any practical system.

2) *Quantum Computing Eavesdropper*: Let us now consider an eavesdropper equipped with a quantum computer, which employs the well-known Grover adaptive search (GAS) algorithm [14] known for its quadratic acceleration of exhaustive searches, shown by state-of-the-art applications in various combinatorial problems in communication systems [15], [16].

The proposed scheme can be shown to be resilient to quantum computing-based eavesdroppers in two-fold. The first is that even under the quadratically-reduced complexity order, the query complexity of the GAS is still $\mathcal{O}(\sqrt{N!})$, which is still combinatorially large for growing N . Secondly, it is known that the number of logical qubits required for the corresponding GAS algorithm is lower-bounded by the base-2 logarithm of the search space size using typical one-hot encoding strategies [17], *i.e.*, $\log_2(N!)$, in addition to the ancillary qubits required to encode the objective function.

Various roadmaps and analyses suggest that quantum computers with 10^3 error-free logical qubits may be expected by 2040, which is approximately the number of qubits required to design the GAS solver of the proposed scheme for $N = 167$. In light of the above, considering that B5G communication systems expect over thousands of subcarriers in higher frequency spectra [1], in addition to the fact that the commercial availability of such large-scale quantum computers may only follow decades after, the proposed scheme is also practically secure against quantum computing-enabled eavesdroppers, unless the quantum computing technology advances extraordinarily beyond current expectations.

B. Eavesdropper with Random Guess Strategy

As the exhaustive search strategy has been shown to be infeasible even via quantum computers, next, we consider the case where the eavesdropper employs a random guess strategy.

1) *Permutation Guessing Probability*: Straightforwardly, the probability of the eavesdropper blindly guessing the correct permutation key k is $\frac{1}{N!}$, which is negligible. However, one must also consider the case where the random guess is very close to the true permutation. In other words, when the guessed permutation of order k' has only ℓ incorrect element positions from the correct permutation of order k .

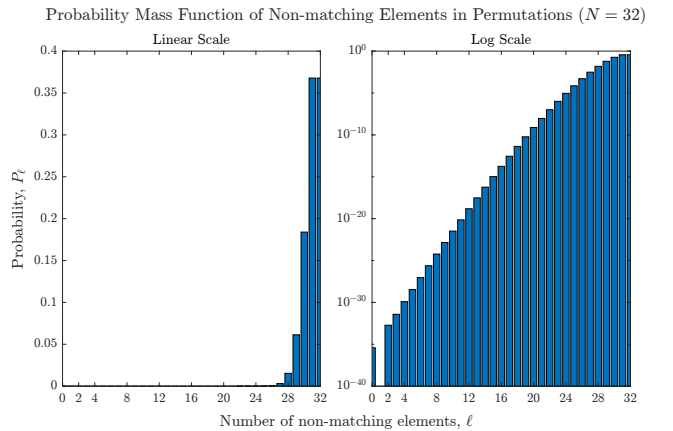


Fig. 2. Probability mass function (PMF) illustrating the probability of a random permutation order k' having ℓ non-matching element positions to a given permutation order k , for a sequence with $N = 32$ number of elements.

Leveraging combinatorial analysis, the number of permutations with ℓ non-matching elements, out of $N!$ total orders, is obtained by considering derangements [18], and is given by

$$D_\ell \triangleq \frac{N!}{\ell!} \sum_{i=0}^{N-\ell} \frac{(-1)^i}{i!}, \quad (18)$$

where D_ℓ represents the total number of permutations with $\ell \in \{0, 1, \dots, N\}$ elements in non-matching positions to a given sequence, with the corresponding probability $P_\ell \triangleq \frac{D_\ell}{N!}$.

In hand of the above, it is possible to obtain the probability mass function (PMF) representing the probability of an eavesdropper guessing a permutation order k' with ℓ number of wrong elements to the true permutation order k . The PMF for a system with $N = 32$ of subcarriers has been illustrated in Figure 2, which highlights the exponentially decreasing probability of the eavesdropper guessing the correct permutation order as the number of wrong elements increases. For example, the probability of the eavesdropper guessing a permutation order with only two wrong positions (closest possible) is $P_{\ell=2} \approx 10^{-33}$, which is negligible. On the other hand, the probability of guessing a completely wrong permutation order (all wrong positions), approaches the asymptotic value of $\lim_{N \rightarrow \infty} P_{\ell=N} = \frac{1}{e} \approx 0.3679$ [18], which is prominent.

2) *BER Performance Analysis*: In light of the above, the detection performance of the eavesdropper with the random guess strategy is analyzed in the following, via numerical simulations considering the BER performance of the MMSE estimator constructed using a random permutation key k' with varying number ℓ of non-matching element positions.

Two sets of numerical results are presented, for the remote eavesdropping (14b) and co-located eavesdropping (17) scenarios respectively, for a system with $N = 32$ subcarriers.

Various cases are investigated, including a random guess, closest possible guess with only two non-matching elements, and the worst-case scenario with all incorrect elements. Of course, the case with only correct guesses is the same as Bob.

TABLE I
RELEVANT SIMULATION PARAMETERS

No. of subcarriers	$N = 32$	No. of scattering paths	$P = 3$
Constellation size	$M = 4$	Max. norm. delay	$\ell^{\max} = 5$
Second chirp freq.	$c_2 = \frac{1}{N\pi}$	Max. norm. Doppler shift	$f^{\max} = 2$

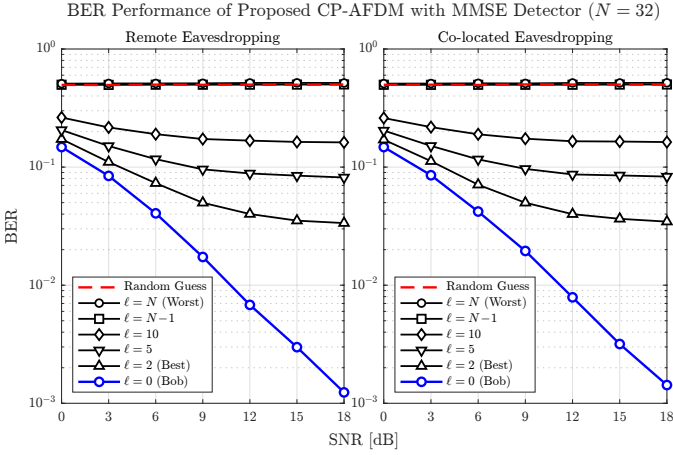


Fig. 3. BER performance of Bob and Eve in a remote (left) and co-located (right) eavesdropping scenario, for various cases of ℓ , with $N = 32$.

Figure 3 illustrates the BER performance of Eve in a remote eavesdropping scenario, *i.e.*, $\mathbf{H}_E \neq \mathbf{H}_B$, and clearly highlights the remarkable security of the proposed scheme, where an eavesdropper with a random guess of the permutation key is completely unable to decode the transmitted data (plotted red).

Even when ideal cases are considered, such as the closest possible guess with $\ell = 2$, which only occurs with the infeasible probability of $P_{\ell=2} \approx 10^{-33}$ for $N = 32$, the communications performance of Eve already degrades from that of Bob, who has the correct permutation key and hence $\ell = 0$. Furthermore, it can be seen that when a moderate number of non-matching elements occur, such as $\ell = 10$, the BER performance of Eve becomes significantly worse than that of Bob, and with completely or mostly wrong orders, such as $\ell = N$ and $\ell = (N - 1)$, the performance is practically the same as a random guess⁴ and therefore undecodable.

In addition, the right subfigure of Figure 3 illustrates the BER performance of Eve in a co-located eavesdropping scenario, as in (17), where Eve has the same CSI as Bob, and therefore receives the exact same signal. It is shown that even in this case, where the security of the scheme is only dependent on the chirp-permutation effect of the proposed scheme, the BER performance of Eve follows the exactly same trend as in the remote eavesdropping scenario, *i.e.*, undecodable when the permutation key k is unknown to the eavesdropper.

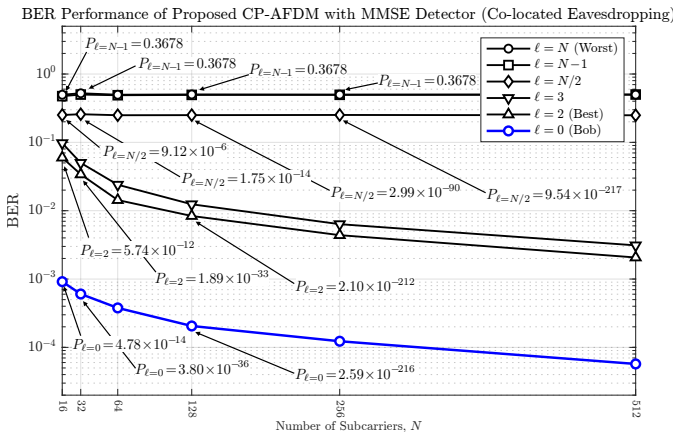


Fig. 4. BER performance of a co-located eavesdropper with the corresponding guessing probabilities, for varying values of ℓ and N , with $\text{SNR} = 18\text{dB}$.

Finally, Figure 4 consolidates the security of the proposed CP-AFDM scheme for larger system sizes with growing number of subcarriers, by illustrating the BER performance of Eve against Bob in a co-located eavesdropping scenario, for various guessing cases ℓ and its corresponding guessing probability. The results highlight that the security of the system is significantly enhanced for larger system sizes, where the probability of the eavesdropper guessing the correct permutation key becomes exponentially smaller, while the BER performance of Eve remains undecodable. For example for $N = 128$, the probability of a correct guess is $P_{\ell=0} = 2.59 \times 10^{-216}$, whereas the closest guess is given by $P_{\ell=2} = 2.10 \times 10^{-211}$.

V. CONCLUSION

We proposed a novel secure communications scheme based on the chirp-permuted AFDM waveform, which provides quantum-resilient physical-layer security against eavesdroppers in a doubly-dispersive channels. It is shown that for eavesdroppers without the secret permutation-order key used by the transmitter, the information is undecodable under random guess strategies, and the classical or quantum computing-based exhaustive search strategies are also infeasible due to the computational hardness and technology requirements.

VI. ACKNOWLEDGEMENT

A part of this work was conducted as part of Project “5G-HyprMesh” (Code 01MO24001C), funded by the Bundesamt für Sicherheit in der Informationstechnik (BSI).

REFERENCES

- [1] W. Jiang *et al.*, “The road towards 6G: A comprehensive survey,” *IEEE Open Journ. ComSoc.*, vol. 2, pp. 334–366, 2021.
- [2] C. Wang *et al.*, “On the road to 6G: Visions, requirements, key technologies, and testbeds,” *IEEE Commun. Surv. Tuts.*, vol. 25, no. 2, 2023.
- [3] H. S. Rou *et al.*, “Integrated sensing and communications for 3D object imaging via bilinear inference,” *IEEE Trans. Wireless Commun.*, 2024.
- [4] L. Mucchi *et al.*, “Physical-layer security in 6G networks,” *IEEE Open Journal of the Communications Society*, vol. 2, pp. 1901–1914, 2021.
- [5] O. Pal *et al.*, “Quantum and Post-Quantum Cryptography,” in *Quant. & Post-Quant. Crypt.*, Wiley, pp. 45–58, 2022.
- [6] S. Vuppala *et al.*, “On the physical layer security analysis of hybrid millimeter wave networks,” *IEEE Trans. Commun.*, vol. 66, no. 3, 2018.
- [7] M. Mitev *et al.*, “What physical layer security can do for 6G security,” *IEEE Open Journ. Veh. Tech.*, vol. 4, pp. 375–388, 2023.
- [8] D. J. Bernstein and T. Lange, “Post-quantum cryptography,” *Nature*, vol. 549, no. 7671, pp. 188–194, 2017.
- [9] M. Kumar, “Post-quantum cryptography algorithm’s standardization and performance analysis,” *Array*, vol. 15, p. 100242, 2022.
- [10] K. Yuki Yoshi *et al.*, “Quantum speedup of the dispersion and codebook design problems,” *IEEE Trans. Quant. Eng.*, vol. 5, pp. 1–16, 2024.
- [11] H. S. Rou *et al.*, “AFDM chirp-permutation-index modulation with quantum-accelerated codebook design,” *IEEE 58th Asilomar Conf. Sig., Sys., Comp.*, 2024.
- [12] A. Bemani *et al.*, “Affine frequency division multiplexing for next generation wireless communications,” *IEEE Trans. Wireless Commun.*, pp. 8214–8229, 2023.
- [13] H. S. Rou *et al.*, “From orthogonal time-frequency space to affine frequency-division multiplexing: A comparative study of next-generation waveforms for integrated sensing and communications in doubly dispersive channels,” *IEEE Sig. Proc. Mag.*, vol. 41, no. 5, pp. 71–86, 2024.
- [14] A. Gilliam *et al.*, “Grover adaptive search for constrained polynomial binary optimization,” *Quantum*, vol. 5, p. 428, 2021.
- [15] K. Yuki Yoshi *et al.*, “Grover adaptive search for maximum likelihood detection of generalized spatial modulation,” in *IEEE 100th Veh. Technol. Conf. Fall*, 2024, pp. 1–5.
- [16] P. Botsinis *et al.*, “Quantum search algorithms for wireless communications,” *IEEE Comm. Surv. Tuts.*, vol. 21, no. 2, pp. 1209–1242, 2018.
- [17] Y. Sano *et al.*, “Accelerating grover adaptive search: Qubit and gate count reduction strategies with higher order formulations,” *IEEE Trans. Quant. Eng.*, vol. 5, pp. 1–12, 2024.
- [18] M. Hassani, “Derangements and applications,” *Journ. Integer Seq.*, vol. 6, no. 1.03.1, 2003.

⁴The probability of choosing a completely wrong order, or an order with only one correct element under a random guess, is $P_{\ell=N} + P_{\ell=N-1} \approx 0.73$, (as shown in Fig. 4), dominating the detection performance.